Nanopatterned rGO/ZnO:Al seed layer for vertical growth of single ZnO nanorods

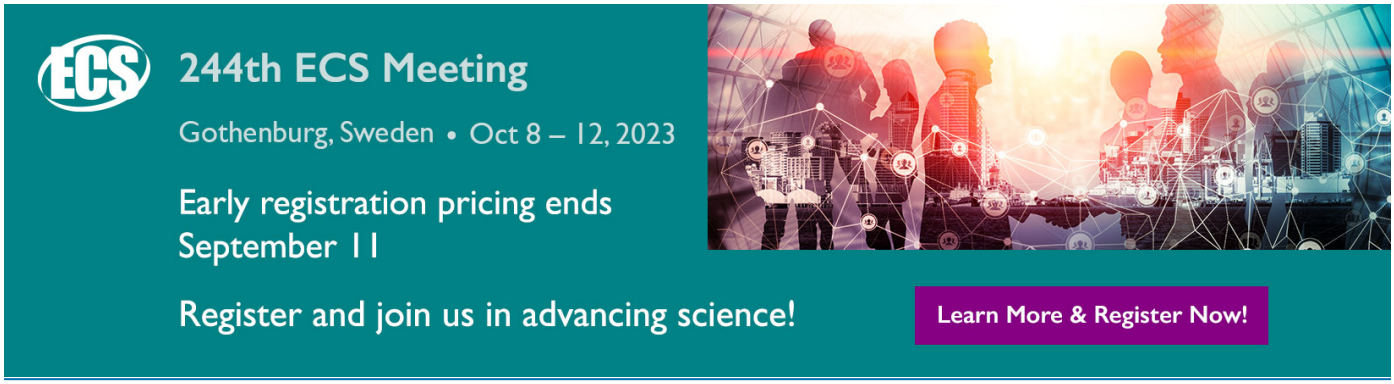

OPEN ACCESS
IOP Publishing
Nanotechnology

Nanotechnology **34** (2023) 255301 (7pp)
https://doi.org/10.1088/1361-6528/acc662

Nanopatterned rGO/ZnO:Al seed layer for vertical growth of single ZnO nanorods

Ebrahim Chalangar[1,2], Elfatih Mustafa[1], Omer Nur[1], Magnus Willander[1] and Håkan Pettersson[1,2,3,*]

[1] Department of Science and Technology, Physics, Electronics and Mathematics, Linköping University, SE-60174 Norrköping, Sweden
[2] School of Information Technology, Halmstad University, Box 823, SE-301 18 Halmstad, Sweden
[3] Solid State Physics and NanoLund, Lund University, Box 118, SE-221 00 Lund, Sweden

E-mail: hakan.pettersson@hh.se

Received 10 November 2022, revised 27 February 2023
Accepted for publication 21 March 2023
Published 11 April 2023

Abstract

In this work, we demonstrate a novel low-cost template-assisted route to synthesize vertical ZnO nanorod arrays on Si (100). The nanorods were grown on a patterned double seed layer comprised of reduced graphene oxide (rGO) and Al-doped ZnO nanoparticles. The seed layer was fabricated by spray-coating the substrate with graphene and then dip-coating it into a Al-doped ZnO sol–gel solution. The growth template was fabricated from a double-layer resist, spin-coated on top of the rGO/ZnO:Al seed layer, and patterned by colloidal lithography. The results show a successful chemical bath deposition of vertically aligned ZnO nanorods with controllable diameter and density in the nanoholes in the patterned resist mask. Our novel method can presumably be used to fabricate electronic devices on virtually any smooth substrate with a thermal budget of 1 min at 300 °C with the seed layer acting as a conductive strain-relieving back contact. The top contact can simply be made by depositing a suitable transparent conductive oxide or metal, depending on the specific application.

Keywords: zinc oxide, nanorod arrays, vertical growth, colloidal lithography, nanofabrication, sol–gel, reduced graphene oxide

(Some figures may appear in colour only in the online journal)

Introduction

A selective-area array of single vertically aligned zinc oxide nanorods (ZnO NRs) on a conductive substrate is highly desirable in many sensing, luminescence, and field-emission device applications. Up to now, many efforts have been made to synthesize ZnO NRs on various substrates, including expensive lattice-matched substrates, e.g., single-crystal ZnO [1], sapphire [2], GaN [3], or more affordable non-epitaxial pre-seeded substrates. For high-quality applications, expensive vacuum or high-temperature deposition techniques such as pulsed laser deposition [4], vapor–liquid–solid (VLS) growth [5], and chemical vapor deposition [6] on single crystalline lattice-matched substrates usually give the best results. However, a high production cost is a major issue for many applications.

During the past two decades, there have been many studies on 1D nanostructured materials for novel electronic and optoelectronic devices, such as light-emitting diodes (LEDs) [7], ultraviolet (UV) detectors [8–10], and biosensors [11]. Among these, ZnO is a promising material due to its wide direct bandgap of 3.2–3.4 eV, large exciton binding energy of 60 meV at room temperature, and excellent piezoelectric properties [12]. Also, in addition to advanced high-temperature growth techniques, simple cost-efficient low-temperature chemical bath deposition (CBD) methods

* Author to whom any correspondence should be addressed.

[13–15] have been deployed for the growth of various interesting morphologies of ZnO.

Efficient CBD of ZnO NRs on strongly lattice-mismatched substrates usually requires a pre-coated polycrystalline seed layer as a nucleation surface [14]. The polarity, size and orientation of the crystalline domains in the seed layer govern the NRs' growth direction and crystal orientation [16]. Therefore, engineering the seed layer crystallinity is a key part of controlling the ZnO NRs orientation.

The polycrystalline seed layers can be deposited with different techniques, e.g., spin-coating, dip-coating, and sputtering. Regardless of the deposition technique used, the deposited seed layer on a non-epitaxial substrate shows randomly distributed crystal particles, leading to a poor *c*-axis alignment of the NRs. This challenge remains even after improving the uniformity of the seed layer and applying post-treatments of the seed layer.

In our previous study [17], highly uniform ZnO seed layers with enlarged crystal grain boundaries of up to 500 nm in lateral size were deposited using a sol–gel technique and subsequently post-sintered at 300 °C for 10 min on a Si (100) substrate. Although the post-treatment of the seed layer improved its smoothness and the size of the crystal boundaries, the desirable (002) crystal plane orientation of the ZnO seed layer did not form. We showed that the crystal structure of the seed layer ultimately depends on the crystallinity of the substrate and the actual lattice mismatch. This dependence on the substrate impairs the desired vertical alignment of the grown ZnO NRs and their usability in various applications.

In this work, we present a new approach for the growth of vertically aligned ZnO NRs on arbitrary mismatched substrates by using a reduced graphene oxide (rGO) buffer layer between the substrate and the ZnO seed layer to compensate for the lattice mismatch, reducing the dependency on the substrate. The electrically conductive rGO buffer layer also serves as a low-resistance back contact, which extends the use of non-conductive substrates for device fabrication. The rGO/ZnO seed layers were prepared by spray-coating a suspension of graphene oxide (GO) flakes on the desired substrate and then dip-coating it into an aluminum-doped ZnO nanoparticle (ZnO:Al NP) sol–gel solution. A subsequent short-time post-annealing step converts the insulating GO to conductive rGO.

In contrast to our previous work, no effort was made here to sinter the ZnO NPs together or to increase their crystallinity. Instead, the rGO/ZnO:Al samples were directly patterned by colloidal lithography (CL), followed by CBD of ZnO NRs. A Si (100) substrate was used in this work; however, our method is independent of the substrate. Additionally, the effect of Al-doping of the ZnO NRs on the electrical properties of the samples was also investigated. Scanning electron microscopy (SEM) and x-ray diffraction (XRD) analyses show a significant improvement in the vertical alignment of the ZnO NRs compared to our previous report on CBD of ZnO NRs on crystallized seed layers. The developed method can be used in different electro-optical applications where a selective area growth of vertically aligned ZnO NRs is required.

Experimental methods

Synthesis of graphene oxide

Graphene oxide (GO) was synthesized using the improved Hummer's method, reported in [18]. Summarized, 1 g of natural graphite flakes, with a particle size range of 150–850 μm, was oxidized in 67 ml of a mixture of 9:1 volume ratio of concentrated H_2SO_4 (98%) and H_3PO_4 (85%) under stirring at 80 °C for 30 min, and ultrasonication for 30 min Subsequently, 6 g of $KMnO_4$ was gently added to the mixture while still stirring and keeping the temperature constant at 0 °C using an ice bath. The mixture was stirred for another 2 h at 35 °C, then diluted by adding 120 ml of DI water, and again stirred for 30 min at 95 °C. The reaction was terminated by adding a solution of 240:3 ml of DI water and H_2O_2 (30%), followed by washing four times using 10% HCl solution in DI water and centrifugation at 4500 rpm for 30 min.

rGO/ZnO:Al seed layer deposition

For deposition of thin GO layers on Si substrates, a two-inch Si (100) wafer was first cleaned by sequential ultrasonication in acetone, isopropanol, and DI water, followed by N_2 blow-drying and heating on a hotplate at 120 °C for 5 min to remove surface moistures. A thin film of the Adhesion Promoter AP3000 (from Advanced Electronics Materials) was spin coated on the substrate at 4000 rpm for 30 s, followed by heating at 120 °C for 10 min. Subsequently, 20 ml of a GO suspension in dimethylformamide (DMF), with a concentration of 2 mg ml^{-1}, was pulse-wise sprayed on the coated substrate while heated on a hotplate at 120 °C under a fume hood. A nitrogen airbrush, kept at a distance of 10 cm from the substrate, operating at a pressure of 2 bar, was used to uniformly deposit GO layers on the substrate in a sequence of pulses of 1 s spraying and 3 s waiting.

An Al-doped ZnO NP sol–gel solution with 2 at% of Al dopants was then prepared by dissolving 375 mM zinc acetate ($Zn(CH_3COO)_2{\cdot}2H_2O$), 7.5 mM aluminum nitrate ($Al(NO_3)_3.9H_2O$), and 375 mM monoethanolamine in 100 ml of pure ethanol, stirred at 60 °C for 10 h and then stirred at room temperature overnight. A thin film of this sol–gel solution was subsequently deposited on the GO-coated substrate by a computer-controlled dip-coater, operating at a speed of 10 mm s^{-1}, and annealed on an infrared hotplate at 300 °C for 1 min under atmospheric conditions. This annealing process partially transforms GO to rGO, exhibiting enhanced conductivity and reduced transparency [19]. Furthermore, the rGO/ZnO:Al NP seed layers were exposed to 254 nm UV irradiation for 10, 30, and 60 min, respectively, to increase their conductivity. We point out here again that this developed rGO/ZnO:Al seed layer deposition method is substrate-independent and expected to work equally well on arbitrary substrates, including non-epitaxial substrates, e.g., glass.

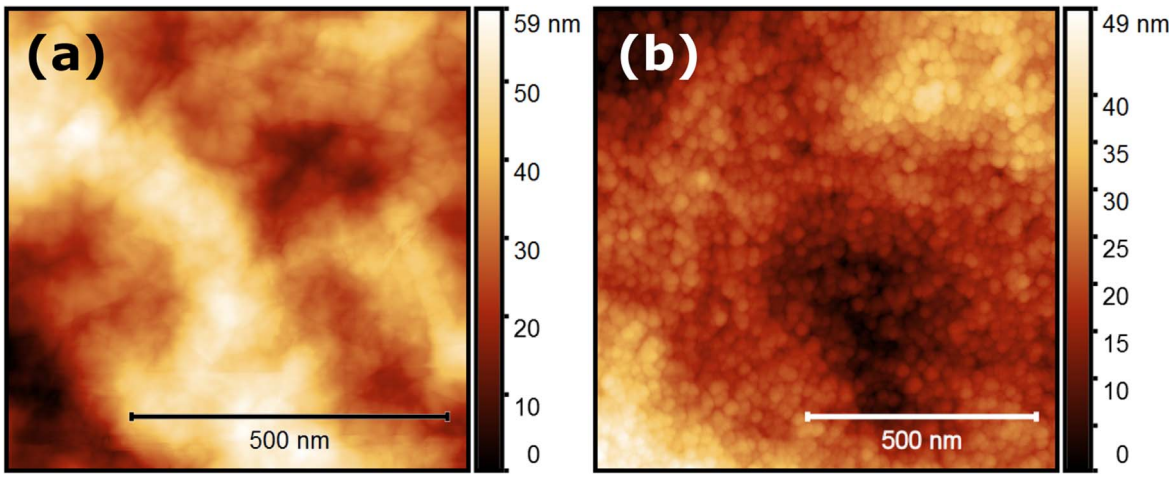

Figure 1. AFM images of (a) a spray-coated GO layer on a Si wafer and (b) a ZnO:Al NP seed layer deposited on top of the spray-coated Si wafer in (a) by the sol–gel and dip-coating methods described above.

Patterning the rGO/ZnO:Al seed layers

The rGO/ZnO:Al seeded substrates were patterned using the CL technique described at length in our recently published report [17]. Briefly explained, double resist layers, comprising a 3 wt% solution of PMMA in toluene and an S1805 positive photoresist, were spin coated on the rGO/ZnO seeded substrates at 4000 rpm for 30 s, followed by soft baking the PMMA layer at 170 °C for 10 min and soft and hard baking the photoresist layer at 110 °C for 30 s and 145 °C for 5 min, respectively. After treating the double resist layer with a 5 min UV-ozone exposure, bettering its hydrophilicity, a 0.2 wt% aqueous solution of poly(diallyldimethylammonium) (PDDA) was pipetted on the samples. After thoroughly rinsing the samples with DI water and drying them with N_2, a 0.1 wt% aqueous suspension of polystyrene nanobeads (PS-NBs) with a mean diameter of 140 nm was drop coated on the samples' surface. Subsequently, a 30 nm thick Al mask was deposited on the samples and patterned by removing the Al-coated PS-NBs using a tapestripping technique. A 90 s reactive-ion etching (RIE), operating at 150 mTorr pressure with 40 sccm O_2 flow and 60 W RF power, opened up the nanoholes in the resist layers down to the ZnO:Al NP seed layer. Finally, the Al mask was wet etched in an aqueous solution of 30 mM KOH and 50 mM $K_3Fe(CN)_6$ at room temperature for 1 min [20], followed by a thorough DI-water rinsing and N_2 blow-drying.

CBD of ZnO NRs on CL-patterned substrates

To grow the ZnO NRs on the CL-patterned rGO/ZnO:Al seed layers, an equimolar chemical bath solution of 50 mM zinc nitrate ($Zn(NO_3)_2{\cdot}6H_2O$) and hexamethylenetetramine (HMT) in 100 ml DI water was prepared. In addition to the growth of undoped ZnO NR samples, ZnO:Al NRs were also synthesized by adding 2 mM aluminum nitrate ($Al(NO_3)_3.9H_2O$) into the growth solution and adjusting the pH to the range of 6–7 by adding ammonia. The prepared substrates were inserted in the chemical bath solution upside down and kept at 95 °C for 2 h to complete the growth.

Results and discussion

Characteristics of the rGO/ZnO:Al seed layer

The smoothness, grain structure, and crystallinity of the seed layer have a vital impact on the alignment and morphology of the grown ZnO NRs. The epitaxial growth of the NRs follows the crystal orientation of the seed layer in each grain domain [21]. This suggests that in any attempt to grow vertically aligned NRs, special attention should be paid to the early stages of the growth process, particularly at the seed layer interface, where the complex growth mechanisms occur.

The smoothness of the seed layer depends on the substrate condition and the deposition method; for instance, perfectly uniform seed layers can be produced using dip-coating and sol–gel techniques. The crystal grain size of the seed layer can be increased at higher temperatures and longer duration of the annealing process, and by increasing the layer's thickness [22]. However, the polar crystallinity of the ZnO seed layer is directly governed by the crystal structure of the substrate and its lattice matching to the seed layer. This limiting factor restricts the available suitable substrates for vertical growth of ZnO NRs to only a few expensive single-crystal candidates, e.g., single-crystalline ZnO [1], sapphire [2], or GaN [3].

Introducing a buffer layer between the ZnO seed layer and the substrate is a possible route to accommodate the lattice mismatch, which in turn opens the possibility of growing vertical NRs on inexpensive arbitrary substrates. Here we used an rGO buffer layer between the ZnO:Al seed layer and the strongly mismatched Si substrates. The 100–150 nm thick spray-coated GO layer formed a uniform large-area surface for the ZnO seed layer deposition. Figure 1(a) shows an atomic force microscopy (AFM) image of the GO surface on a Si substrate with an RMS roughness of 11 nm. A silane coating under the GO layer improved its adhesion to the substrate enough to leave it intact during the subsequent CL steps, including tape-stripping of the NBs.

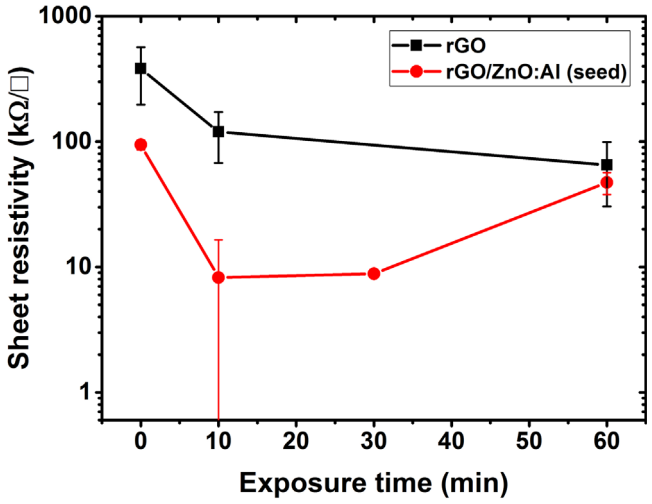

Figure 2. Variation of the sheet resistivity with the UV exposure time of rGO and rGO/ZnO:Al seed layers deposited on glass substrates by spray-coating and dip-coating, respectively. The resistivities are measured using the four-point probe technique after annealing at 300 °C for 1 min.

Figure 1(b) shows an AFM image of the ZnO:Al NP seed layer formed by dip-coating the GO-coated Si substrate in the Al-doped ZnO sol–gel solution after annealing. Evidently, the surface RMS roughness improved to around 8 nm. As mentioned before, the annealing process was limited to only 1 min at 300 °C under atmospheric conditions to avoid burning the GO layer. Our findings show that a longer annealing time, or even annealing in an inert ambient, leads to the total removal of the GO layer due to the existing surface oxygen groups on the GO and ZnO layers. As readily observed in figure 1(b), one-minute annealing is insufficient to entirely sinter the ZnO NPs together to form larger crystal grains. This conclusion is also corroborated by the absence of any observed specific crystal orientation detected by XRD analysis.

Although the rGO/ZnO:Al seed layer showed a relatively low sheet resistivity of about 100 kΩ/□, exposure to UV irradiation further enhanced its conductivity by one order of magnitude. Figure 2 shows the sheet resistivity of rGO and rGO/ZnO:Al seed layers after 60 min irradiation by UV light. It has been demonstrated that UV treatment improves the conductivity of ZnO [23]. Moreover, photoexcited electrons in the conduction band of ZnO are injected into the GO layer, causing a stronger GO reduction to rGO, which in turn leads to higher conductivity [24]. The minimum resistivity was achieved after 10 min irradiation.

CL-patterned seed layers

An array of nanoholes was formed on the prepared rGO/ZnO:Al seed layers using the CL technique described above. The top-view SEM image in figure 3(a) shows a uniform distribution of the etched nanoholes in the resist layer. Using 140 nm-diameter PS-NBs resulted in a nanohole diameter distribution centered around 170 nm (figure 3(b)) and a surface density of 6.1 nanoholes μm^{-2}. Although the pattern seems randomly distributed at first glance, the radial distribution function in figure 3(c) reveals two lateral ordering periods with distances of 319 nm and 750 nm, respectively, between two first neighbor hole centers. This short-range order stems from net repulsive forces between the negatively charged PS-NBs.

CBD-grown ZnO NRs on CL-patterned Si substrates

After the CBD of ZnO NRs on the CL-patterned rGO/ZnO:Al NP seed layers deposited on Si substrates, the morphology and the crystalline structure of the final structures were investigated by SEM and XRD analysis. Figures 4(a)–(c) show SEM images of the grown ZnO NRs from different views. The growth mechanism can be described as a sequence of stages where, initially, the growth solution penetrates into the nanoholes in the resist layer and reaches the hydrophilic ZnO seed layer. It is crucial to have an optimal opening diameter for single NR growth in each nanohole. The small-size nanoholes are difficult to penetrate by the growth solution due to the hydrophobicity of the resist layer, while the large-size nanoholes lead to disordered multiple NR growth in different directions. After careful evaluation, 140 nm diameter PS-NBs were finally selected based on the resulting growth results.

Next, in the absence of crystalline grain domains, the seed layer provides random nuclei sites causing texture-controlled epitaxial growth of ZnO NRs. A gradual transition from a texture morphology to a *c*-axis crystal orientation takes place within the 200 nm thickness of the resist layer, where the growth of off-directional NRs is blocked by the nanohole walls, resulting in near-vertical ZnO NRs with a *c*-axis orientation.

A significant improvement in the vertical alignment of the present ZnO NRs, compared to two other sets of NRs recently reported by our group, was furthermore confirmed by statistical analyses of SEM images and XRD data. Figure 4(d) shows the distribution of deviation angles from the surface normal of NRs in the SEM image in figure 4(a). The extracted mean deviation angle amounts to 7°, which is significantly smaller than our previously reported 13° and 18° for CL-patterned crystallized and non-patterned crystallized seed layers [17].

Figure 5 shows diffractograms of three different samples, the present sample, ZnO NRs grown on a CL-patterned crystallized ZnO NP seed layer, and ZnO NRs grown on a non-patterned ZnO NP seed layer [17], respectively. Here, the observed pronounced (002) reflections, originating from the *c*-axis crystal planes of ZnO, compared to (100) and (101) reflections, show that our novel patterned rGO/ZnO:Al seed layer leads to a significantly improved vertical growth of ZnO NRs. This improvement is readily observed by comparing the SEM images in this work with those in [17].

To investigate the effect of Al-doping on the ZnO NRs' conductivity, a 30 nm thick Al top contact was thermally evaporated on the top and sidewalls of the ZnO NRs, with and without Al-doping. Figure 6 shows symmetric *J*–*V* characteristics measured between the Al top contact and the bottom rGO/ZnO:Al seed layer. The *J*–*V* data were acquired at

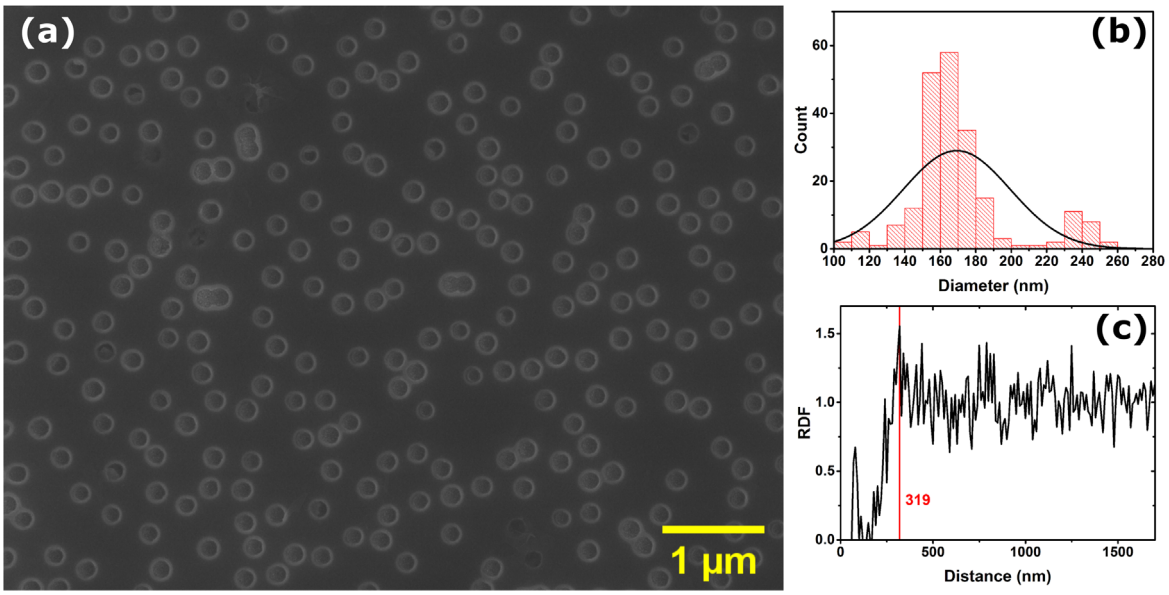

Figure 3. (a) SEM image of a nanohole array in a resist layer on top of an rGO/ZnO:Al seed layer. CL patterning was performed using 140 nm diameter PS-NBs. (b) Distribution of the diameter of the patterned nanoholes with a central diameter of 170 nm. (c) The radial distribution function of the spacing between the nanoholes with a first peak density at 319 nm and a secondary lower peak density at 750 nm.

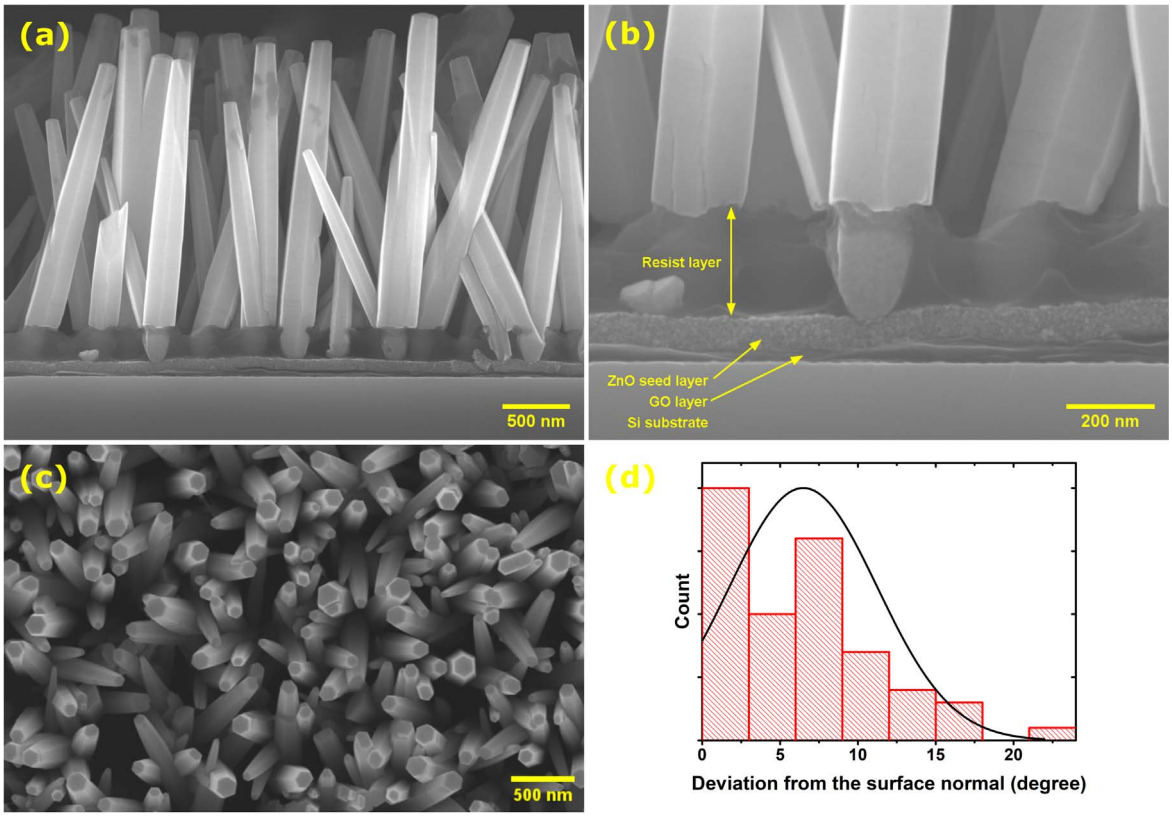

Figure 4. SEM images of CBD-grown ZnO NRs on an optimized CL-patterned rGO/ZnO:Al seed layer, deposited on a Si (100) substate at (a) low magnification and (b) high magnification in cross-sectional and (c) top views. (d) Distribution of the deviation angles from the surface normal with a mean deviation angle of 7°, calculated from the cross-sectional SEM image in (a). Each nanohole in the resist layer contains a single ZnO NR.

room temperature with a Keithley 4200-SCS, operating in a linear voltage sweep mode from −2 to 2 V range with steps of 40 mV. The results show two orders of magnitude increase in the conductivity of ZnO:Al NRs compared to undoped NRs. It also shows that efficient charge transfer occurs at the Si-rGO and rGO-ZnO interfaces, and that the resist layer has perfectly isolated the substrate from the upper medium. Our disruptive method can presumably be used to fabricate ZnO

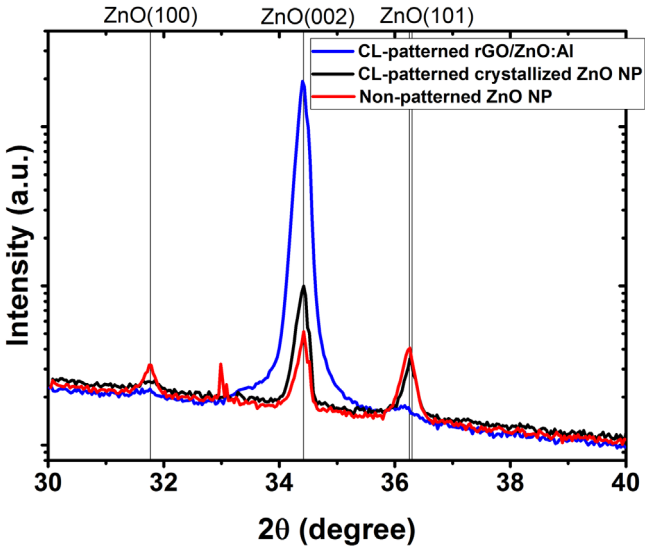

Figure 5. XRD diffractograms of CBD-grown ZnO NRs on a CL-patterned rGO/ZnO:Al NP seed layer (this work), a CL-patterned crystallized ZnO NP seed layer annealed for a long time, and a non-patterned ZnO NP seed layer. The last two graphs were reprinted from [17] under a CC BY 4.0 license.

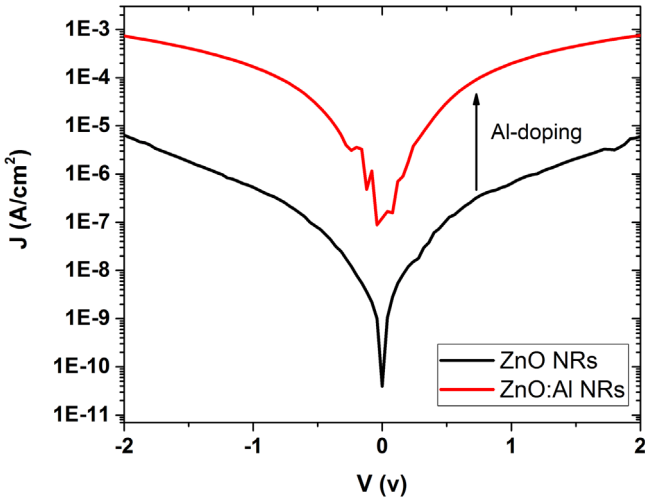

Figure 6. *J*–*V* characteristics of CBD-grown ZnO NRs, with and without Al doping, on CL-patterned rGO/ZnO:Al seed layers on n-type Si substrates, measured in darkness at room temperature.

NR-based electronic devices on virtually any smooth substrate with a thermal budget of 1 min at 300 °, with the seed layer acting as a conductive strain-relieving back contact and a top contact of a suitable transparent conductive oxide, or metal, depending on the specific application.

Conclusions

Summarized, we demonstrate a novel low-cost route to fabricate high-quality undoped and Al-doped ZnO nanorods on Si (100) substrates. The nanorods were grown on a patterned conductive and strain-relieving double seed layer of reduced graphene oxide and Al-doped ZnO nanoparticles deposited on the Si substrates. Subsequently, a growth mask was fabricated from a resist layer patterned by colloidal lithography. Chemical bath deposition was used to synthesize single high-quality vertical nanorods in each of the designated nanoholes in the resist template. Our method can presumably be used to fabricate novel high-quality ZnO nanorod-based optoelectronic devices on virtually any substrate offering a thermal budget of 1 min at 300 °C, with the seed layer acting as a conductive strain-relieving back contact and an additional suitable top contact.

Data availability statement

All data that support the findings of this study are included within the article (and any supplementary files).

Declarations

Competing interests

The authors declare that they have no competing interests.

Funding

This research was funded by the ÅForsk Foundation (project number 19–725).

Authors' contributions

EC conceived the research idea, prepared and characterized all samples, and wrote the original draft. EC and HP analyzed the data. EM performed the CBD, XRD analysis and edited the first draft. All authors read, revised, and approved the final manuscript.

ORCID iDs

Ebrahim Chalangar https://orcid.org/0000-0002-6850-1552
Elfatih Mustafa https://orcid.org/0000-0002-8985-0604
Omer Nur https://orcid.org/0000-0002-9566-041X
Magnus Willander https://orcid.org/0000-0001-6235-7038
Håkan Pettersson https://orcid.org/0000-0001-5027-1456

References

[1] Consonni V, Sarigiannidou E, Appert E, Bocheux A, Guillemin S, Donatini F, Robin I-C, Kioseoglou J and Robaut F 2014 Selective area growth of well-ordered ZnO

nanowire arrays with controllable polarity *ACS Nano* **8** 4761–70
[2] Erdélyi R, Nagata T, Rogers D J, Teherani F H, Horváth Z E, Lábadi Z, Baji Z, Wakayama Y and Volk J 2011 Investigations into the impact of the template layer on ZnO nanowire arrays made using low temperature wet chemical growth *Cryst. Growth Des.* **11** 2515–9
[3] Xu S, Wei Y, Kirkham M, Liu J, Mai W, Davidovic D, Snyder R L and Wang Z L 2008 Patterned growth of vertically aligned ZnO nanowire arrays on inorganic substrates at low temperature without catalyst *J. Am. Chem. Soc.* **130** 14958–9
[4] Rahman F 2019 Zinc oxide light-emitting diodes: a review *Opt. Eng.* **58** 010901
[5] Gomez J L and Tigli O 2013 Zinc oxide nanostructures: from growth to application *J. Mater. Sci.* **48** 612–24
[6] Müller R, Huber F, Gelme O, Madel M, Scholz J-P, Minkow A, Herr U and Thonke K 2019 Chemical vapor deposition growth of zinc oxide on sapphire with methane: initial crystal formation process *Cryst. Growth Des.* **19** 4964–9
[7] Qian F, Li Y, Gradečak S, Wang D, Barrelet C J and Lieber C M 2004 Gallium nitride-based nanowire radial heterostructures for nanophotonics *Nano Lett.* **4** 1975–9
[8] Sang L, Liao M and Sumiya M 2013 A comprehensive review of semiconductor ultraviolet photodetectors: from thin film to one-dimensional nanostructures *Sensors* **13** 10482–518
[9] Kind H, Yan H, Messer B, Law M and Yang P 2002 Nanowire ultraviolet photodetectors and optical switches *Adv. Mater.* **14** 158–60
[10] Dai W, Pan X, Chen S, Chen C, Wen Z, Zhang H and Ye Z 2014 Honeycomb-like NiO/ZnO heterostructured nanorods: photochemical synthesis, characterization, and enhanced UV detection performance *J. Mater. Chem.* C **2** 4606–14
[11] Tripathy N and Kim D-H 2018 Metal oxide modified ZnO nanomaterials for biosensor applications *Nano Converg.* **5** 27
[12] Desai A V and Haque M A 2007 Mechanical properties of ZnO nanowires *Sensors Actuators Phys.* **134** 169–76
[13] Cadafalch Gazquez G, Lei S, George A, Gullapalli H, Boukamp B A, Ajayan P M and ten Elshof J E 2016 Low-cost, large-area, facile, and rapid fabrication of aligned ZnO nanowire device arrays *ACS Appl. Mater. Interfaces* **8** 13466–71
[14] Greene L E, Law M, Tan D H, Montano M, Goldberger J, Somorjai G and Yang P 2005 General route to vertical ZnO nanowire arrays using textured ZnO seeds *Nano Lett.* **5** 1231–6
[15] Xu S and Wang Z L 2011 One-dimensional ZnO nanostructures: Solution growth and functional properties *Nano Res.* **4** 1013–98
[16] Cossuet T, Roussel H, Chauveau J-M, Chaix-Pluchery O, Thomassin J-L, Appert E and Consonni V 2018 Well-ordered ZnO nanowires with controllable inclination on semipolar ZnO surfaces by chemical bath deposition *Nanotechnology* **29** 475601
[17] Chalangar E, Nur O, Willander M, Gustafsson A and Pettersson H 2021 Synthesis of vertically aligned ZnO nanorods using sol–gel seeding and colloidal lithography patterning *Nanoscale Res. Lett.* **16** 46
[18] Marcano D C, Kosynkin D V, Berlin J M, Sinitskii A, Sun Z, Slesarev A, Alemany L B, Lu W and Tour J M 2010 Improved synthesis of graphene oxide *ACS Nano* **4** 4806–14
[19] Wassei J K and Kaner R B 2010 Graphene, a promising transparent conductor *Mater. Today* **13** 52–9
[20] Vellekoop M J, Visser C C O, Sarro P M and Venema A 1990 Compatibility of zinc oxide with silicon IC processing *Sensors Actuators Phys.* **23** 1027–30
[21] Consonni V and Lord A M 2021 Polarity in ZnO nanowires: a critical issue for piezotronic and piezoelectric devices *Nano Energy* **83** 105789
[22] Nian Q, Callahan M, Look D, Efstathiadis H, Bailey J and Cheng G J 2015 Highly transparent conductive electrode with ultra-low HAZE by grain boundary modification of aqueous solution fabricated alumina-doped zinc oxide nanocrystals *APL Mater.* **3** 062803
[23] Edinger S, Bansal N, Bauch M, Wibowo R A, Hamid R, Trimmel G and Dimopoulos T 2017 Comparison of chemical bath-deposited ZnO films doped with Al, Ga and In *J. Mater. Sci.* **52** 9410–23
[24] Adam R E, Chalangar E, Pirhashemi M, Pozina G, Liu X, Palisaitis J, Pettersson H, Willander M and Nur O 2019 Graphene-based plasmonic nanocomposites for highly enhanced solar-driven photocatalytic activities *RSC Adv.* **9** 30585–98